Nearly resonant multidimensional systems under a transient perturbative interaction

Antonia Ruiz,[1] José P. Palao,[2] and Eric J. Heller[3]
[1]*Departamento de Física Fundamental y Experimental, Electrónica y Sistemas and IUdEA, Universidad de La Laguna, La Laguna 38204, Spain*
[2]*Departamento de Física Fundamental II and IUdEA, Universidad de La Laguna, La Laguna 38204, Spain*
[3]*Departments of Chemistry and Physics, Harvard University, Cambridge, Massachusetts 02138, USA*
(Received 11 August 2009; published 23 December 2009)

We analyze the response of a classical system with $N \geq 2$ internal degrees of freedom satisfying $R \leq (N-1)$ approximated resonance conditions to an external perturbative transient interaction. Under certain assumptions on the system internal frequencies and on the coupling interaction, we show the precise $N-R$ adiabatic invariants and obtain an estimate of the span of the domain defined by the intersecting resonances. The results are illustrated considering a system of three anharmonic oscillators transiently coupled by an explicitly time-dependent interaction, and applied to the low energy vibro-rotationally inelastic collisions between two diatomic molecules.

DOI: 10.1103/PhysRevE.80.066606 PACS number(s): 45.20.−d, 05.45.−a

I. INTRODUCTION

The response of an N-dimensional integrable system to a weak perturbation is strongly conditioned by its internal dynamics and the strength, form, and duration of the external interaction. The dynamics of a system with initial frequencies in the proximity of R independent resonance conditions may be characterized by the presence of $N-R$ adiabatic invariants [1]. In general, the size of the multiple resonance domain bearing such invariants is very small due to the massive activation of high order resonances by the interaction. However, for weak transient interactions with duration long enough to activate the response of small order resonances but short to prevent the effects of high order resonances, the multiple resonance domain may extend over a significant range of initial conditions. In this case, the existence of adiabatic invariants during the time evolution implies that some propensity rules relating the changes in the internal action variables are extremely well preserved within such intervals. These propensity rules correlate the initial and final states of the system.

This effect is well understood in two-dimensional integrable systems, in which only a single resonance condition can be activated by the transient interaction for a given set of initial conditions. A nice illustration is the experimental observation of remarkably sharp strong peaks in the vibro-rotational inelastic rate constant of state resolved low velocity inelastic collisions between atoms and vibro-rotationally excited diatom molecules [2,3]. In this system, nearly resonant vibrational and rotational molecular degrees of freedom are strongly coupled by the transient interaction with the colliding atom, over significant ranges of initial internal molecular states. Within these intervals, an specific correlation between the changes in the vibrational and rotational quantum numbers exists. It was shown that a fully classical treatment reproduces these experimental results remarkably well [3–5].

Another interesting illustration is the observation of significant nonspecular peaks in the quantum diffraction spectrum of grazingly incident fast atoms scattered from a periodic surface, for incident beams closely aligned to an index direction on the surface [6–10]. In this process the adiabatic invariant is the momentum component along the index direction [11,12]. The peaks in the quantum diffraction spectrum reflect a significant momentum exchange between the two momentum components perpendicular to the index direction. A classical analysis predicts that the interval of incidence conditions around the index direction for which the quantum diffraction patterns survive approximately corresponds to the spectrum width [12].

Classically, these effects arising in nearly resonant two-dimensional integrable systems perturbed by some external transient interaction can be explained in terms of the canonical perturbation theory and the method of averaging [1,13]. The first application of this approach to the vibration-rotation transfer in atom-diatom scattering was proposed in Ref. [14]. Since then, the classical analysis of the dynamics of two-dimensional integrable systems in the proximity of a single isolated resonance condition and under a transient interaction has been made precise and applied to different processes, such as the coupling of two anharmonic oscillators by an explicitly time-dependent interaction [15], the low energy vibro-rotationally inelastic atom-diatom collisions [16], and the atom-surface grazing collisions [11,12]. In the context of atom-diatom collisions, the response of the nearly resonant molecule to the transient interaction was named "quasiresonant energy transfer," to stress that the correlated variables are the changes in the vibrational and rotational actions, more than in the energies [2]. By extension, this effect has been called "quasiresonance" in the general analysis of two-dimensional systems [11,12,15,16]. However, we will use the term "nearly resonant" to stress that the effect is associated with approximated resonance conditions satisfied by the initial internal frequencies of the system.

In this work we extend the classical analysis on two-dimensional integrable systems to transient interactions acting on systems with $N \geq 2$ internal degrees of freedom in the proximity of $R \leq (N-1)$ overlapping resonance conditions. The possible overlap of resonance conditions, absent in the two-dimensional analysis, may lead to a whole family of propensity rules involving more than two action variables.

 ©2009 The American Physical Society

This general analysis allows to examine new processes such as the molecule-molecule collisions. The paper is organized as follows. In Sec. II we derive the specific form of the adiabatic invariants and the general expression given all the possible propensity rules arising within a multiple resonance domain. Section III presents the estimate of the span of this domain for intersecting resonances. In Sec. IV the theory is illustrated considering a model of three anharmonic oscillators that are transiently coupled by a time-dependent interaction. The low energy collisions between two diatom molecules are analyzed in Sec. V. Finally, Sec. VI summarizes the main results.

II. ADIABATIC INVARIANTS IN NEARLY RESONANT MULTIDIMENSIONAL SYSTEMS

We consider a N-dimensional integrable system H_0 described by the N action variables $\mathbf{J}=(J_1,\ldots,J_N)$ and their conjugated angles $\mathbf{\Phi}=(\Phi_1,\ldots,\Phi_N)$. The frequencies $\boldsymbol{\omega}=(\omega_1,\ldots,\omega_N)$ of this unperturbed system are given by the relation

$$\dot{\Phi}_i = \frac{\partial H_0}{\partial J_i} = \omega_i(\mathbf{J}). \tag{1}$$

The system is perturbed by a weak transient interaction $\varepsilon V(\mathbf{\Phi},\mathbf{Q},t)$, where $\mathbf{Q}=(Q_1,\ldots,Q_K)$ denote K possible additional external degrees of freedom in the global system, not necessarily given in action-angle variables. The weak character of this interaction is made explicit by considering a perturbative parameter ε. This general expression includes as a particular case autonomous transient interactions for which V does not depend explicitly on time and the transient nature of the interaction is given by the decay of the potential strength for asymptotic values of the coordinates $\mathbf{Q}$. The Hamiltonian describing the total system is then

$$H = H_0(\mathbf{J}) + H_1(\mathbf{Q},\mathbf{P}) + \varepsilon V(\mathbf{\Phi},\mathbf{Q},t), \tag{2}$$

where H_1 is the Hamiltonian of the "external" degrees of freedom, and $\mathbf{P}=(P_1,\ldots,P_K)$ are the conjugate momenta of the coordinates $\mathbf{Q}$. A most general potential also depending on the actions $\mathbf{J}$ could be considered. In that case the analysis presented below is valid provided all the system frequencies $\omega_i \gg \varepsilon \partial V/\partial J_i$.

The perturbative transient interaction induces a process in the system H_0, which changes from an initial state with action values $\mathbf{J}_0$ to a final state with action values $\mathbf{J}_f$ once the interaction is switched off. We assume that (i) the initial state satisfies $R<N$ independent approximated resonance conditions given by the R commensurate relations

$$\mathbf{M}^{(i)} \cdot \boldsymbol{\omega} = \sum_{j=1}^{N} M_j^{(i)} \omega_j(\mathbf{J}_0) \approx 0, \tag{3}$$

with $i=1,\ldots,R$ and $M_j^{(i)}$ integers, i.e., the initial state is within the multiple resonance domain defined by the overlap of the domains associated with the not necessarily intersecting single resonance conditions. The rank of the matrix with elements $M_{ij}=M_j^{(i)}$ is equal to R. From now on, we sort the frequencies $\omega_j(\mathbf{J}_0)$ according to the following two conditions: (a) the minor M_{ij}, with $i,j=1,\ldots,R$, has a nonzero determinant and (b) the absolute value of frequencies ω_l, with $l=R+1,\ldots,N$, are the largest possible compatible with condition (a). The perturbative analysis below is based on ω_l being far enough from zero. Besides, we assume that (ii) the "external" coordinates $\mathbf{Q}$ are slow compared with the angles Φ_l, $l=R+1,\ldots,N$, and (iii) the interaction potential V is a smooth function of its arguments.

To analyze the dynamics of the perturbed system in the proximity of the R resonance conditions, we consider a point transformation from the original action-angle variables $(\mathbf{J},\mathbf{\Phi})$ to a new set $(\mathbf{I},\boldsymbol{\phi})$, $\mathbf{I}=(I_1,\ldots,I_N)$ and $\boldsymbol{\phi}=(\phi_1,\ldots,\phi_N)$, given by the generating function

$$F(\mathbf{I},\mathbf{\Phi},\mathbf{Q},\mathbf{P}) = \sum_{i=1}^{R}\left(\sum_{j=1}^{N} M_j^{(i)}\Phi_j\right) I_i + \sum_{i=R+1}^{N} \Phi_i I_i + \sum_{i=1}^{K} Q_i P_i. \tag{4}$$

The coordinates $\mathbf{Q}$ and their conjugate momenta $\mathbf{P}$ remain unchanged under this transformation. The transformation determines the new angle variables,

$$\phi_i = \frac{\partial F}{\partial I_i} = \begin{cases} \displaystyle\sum_{j=1}^{N} M_j^{(i)}\Phi_j, & 1 \le i \le R \\ \Phi_i, & R+1 \le i \le N, \end{cases} \tag{5}$$

and the relation between the original and the new actions,

$$J_i = \frac{\partial F}{\partial \Phi_i} = \begin{cases} \displaystyle\sum_{j=1}^{R} M_i^{(j)} I_j, & 1 \le i \le R \\ \displaystyle\sum_{j=1}^{R} M_i^{(j)} I_j + I_i, & R+1 \le i \le N. \end{cases} \tag{6}$$

From these last equations, the new actions $\mathbf{I}$ can be expressed in terms of the original actions $\mathbf{J}$,

$$\mathbf{I} = \mathcal{M}^{-1} \cdot \mathbf{J}, \tag{7}$$

with $\mathcal{M}$ the matrix of elements

$$\mathcal{M}_{ij} = \begin{cases} M_i^{(j)}, & 1 \le i \le N;\ 1 \le j \le R \\ 0, & 1 \le i \le R;\ R+1 \le j \le N \\ \delta_{ij}, & R+1 \le i \le N;\ R+1 \le j \le N. \end{cases} \tag{8}$$

The transformed Hamiltonian is then

$$\bar{H} = \bar{H}_0(\mathbf{I}) + H_1(\mathbf{Q},\mathbf{P}) + \varepsilon \bar{V}(\boldsymbol{\phi},\mathbf{Q},t), \tag{9}$$

and the time evolution of the new angles can be obtained as

$$\dot{\phi}_i = \frac{\partial \bar{H}}{\partial I_i} = \begin{cases} \displaystyle\sum_{j=1}^{N} M_j^{(i)}\omega_j, & 1 \le i \le R \\ \omega_i, & R+1 \le i \le N. \end{cases} \tag{10}$$

Using the approximately resonance conditions Eq. (3), $\dot{\phi}_i \approx 0$ for $i=1,\ldots,R$. Under the assumptions (i) and (ii), the angles ϕ_j, $j=R+1,\ldots,N$, oscillate much more rapidly than both the rest of internal angles ϕ_i, $i=1,\ldots,R$, and the "ex-

ternal" coordinates Q_l. Besides, the time derivatives of the new actions,

$$\dot{I}_j = -\frac{\partial \bar{H}}{\partial \phi_j} = -\varepsilon \frac{\partial \bar{V}}{\partial \phi_j}, \tag{11}$$

are small as a consequence of assumption (iii), indicating that the actions I_j are also slow. Therefore the dynamics of the perturbed system in the proximity of the R resonance conditions can be described by averaging the Hamiltonian Eq. (9) over the fast oscillating angles, resulting in

$$\bar{H}' = \bar{H}_0(\mathbf{I}) + H_1(\mathbf{Q},\mathbf{P}) + \varepsilon \bar{V}'(\phi_1, \ldots, \phi_R, \mathbf{Q}, t), \tag{12}$$

where

$$\bar{V}'(\phi_1, \ldots, \phi_R, \mathbf{Q}, t) = \frac{1}{(2\pi)^{N-R}} \prod_{j=R+1}^{N} \int_0^{2\pi} d\phi_j \bar{V}(\phi, \mathbf{Q}, t). \tag{13}$$

Since the angles ϕ_i, $i=R+1,\ldots,N$ are cyclic in the averaged Hamiltonian $\bar{H}'$, their corresponding $N-R$ conjugated actions I_i are adiabatic invariants in the evolution of the perturbed system during the whole transient process, $\Delta I_i = I_{fi} - I_{0i} \approx 0$. According to Eq. (7), the adiabatic invariance of the actions I_i, $i=R+1,\ldots,N$, leads to $N-R$ relations for the changes in the actions $\mathbf{J}$,

$$\sum_{j=1}^{N} [\mathcal{M}^{-1}]_{ij} \Delta J_j \approx 0. \tag{14}$$

They can be combined to give up to

$$N_{\text{rules}} = \begin{pmatrix} N \\ R+1 \end{pmatrix} \tag{15}$$

different (but not independent) propensity rules relating the changes in the original actions $\mathbf{J}$. These N_{rules} relations can be obtained from the general expression

$$\sum_{i_1=1}^{N} \cdots \sum_{i_{R+1}=1}^{N} \epsilon_{i_1,\ldots,i_{R+1},i_{R+2},\ldots,i_N} M_{i_1}^{(1)} \ldots M_{i_R}^{(R)} \Delta J_{i_{R+1}} \approx 0, \tag{16}$$

with $i_{R+2},\ldots,i_N = 1,\ldots,N$ and $\epsilon_{i_1,\ldots,i_{N_R+1},i_{N_R+2},\ldots,i_N}$ the isotropic tensor of rank N. This general expression including all the possible propensity rules indicates that the wedge product

$$\mathbf{M}^{(1)} \wedge \ldots \wedge \mathbf{M}^{(R)} \wedge \Delta\mathbf{J} \approx 0 \tag{17}$$

during the time evolution of the perturbed system in the proximity of the R resonance conditions. The expression Eq. (17) is satisfied if and only if the $R+1$ vectors $\mathbf{M}^{(i)}$, $i=1,\ldots,R$, and $\Delta\mathbf{J}$ are linearly dependent. Therefore the vector of the action changes $\Delta\mathbf{J}$ can be expressed in terms of the resonance vectors as

$$\Delta\mathbf{J} \approx \sum_{i=1}^{R} \mu_i \mathbf{M}^{(i)}, \tag{18}$$

with all the scalars $\mu_i \neq 0$. Consequently, according to the multiple resonance conditions Eq. (3), the internal energy of the nearly resonant perturbed system is approximately constant during the transient process, i.e.,

$$\Delta E_i \approx \boldsymbol{\omega} \cdot \Delta\mathbf{J} \approx \sum_{i=1}^{R} \mu_i (\boldsymbol{\omega} \cdot \mathbf{M}^{(i)}) \approx 0. \tag{19}$$

Two illustrative examples are: (a) The dynamics of a perturbed system in the proximity of a single resonance ($R=1$) presents $N-1$ adiabatic invariants leading to $N_{\text{rules}} = N(N-1)/2$ propensity rules given by

$$\sum_{i_1=1}^{N} \sum_{i_2=1}^{N} \epsilon_{i_1,i_2,i_3,\ldots,i_N} M_{i_1}^{(1)} \Delta J_{i_2} \approx 0, \tag{20}$$

with $i_3,\ldots,i_N = 1,\ldots,N$, or by the single expression $\mathbf{M}^{(1)} \wedge \Delta\mathbf{J} \approx 0$, which indicates that the change in the actions occurs along the direction given by the resonance vector, $\Delta\mathbf{J} \approx \mu_1 \mathbf{M}^{(1)}$. (b) The time evolution in the proximity of $R = N-1$ resonances presents a single adiabatic invariant leading to an unique propensity rule,

$$\sum_{i_1=1}^{N} \cdots \sum_{i_N=1}^{N} \epsilon_{i_1,\ldots,i_N} M_{i_1}^{(1)} \ldots M_{i_{N-1}}^{(N-1)} \Delta J_{i_N} \approx 0, \tag{21}$$

involving the changes in all the internal actions $\mathbf{J}$. This equation can also be expressed as the wedge product $\mathbf{M}^{(1)} \wedge \cdots \wedge \mathbf{M}^{(N-1)} \wedge \Delta\mathbf{J} \approx 0$.

In general all the actions I_i, $i=1,\ldots,R$, can change during the transient perturbation. However, it could happen that the transformed potential $\bar{V}$ in Eq. (9) does not depend on some of the angles ϕ_i. In such cases, the corresponding actions I_i would be additional invariants of the motion. Also, if the averaged potential Eq. (13) does not depend on some of the angles ϕ_i, the actions I_i will be adiabatic invariants. In both cases, new relations similar to Eq. (14) would be obtained.

III. SIZE OF THE DOMAIN FOR INTERSECTING RESONANCES

To obtain an estimate of the size, we restrict the analysis to multiple resonance domains defined by the intersection of several resonance conditions in processes occurring from initial states with the same internal energy $E_0 = H_0(\mathbf{J}_0)$. We assume that the resonance zone remains isolated in phase space throughout the interaction, reaching its maximum size at maximum interaction strength. With this assumption, the duration of the transient process is not relevant in the analysis.

In the action space $\mathbf{J}$, the energy surface has dimensionality $N-1$. A resonance condition $\mathbf{M} \cdot \boldsymbol{\omega} = 0$ also defines a surface of dimensionality $N-1$, meanwhile R simultaneous resonance conditions, $\mathbf{M}^{(i)} \cdot \boldsymbol{\omega} = 0$, $i=1,\ldots R$, define a $N-R$ dimensional surface. Therefore the intersection of the energy and the multiple resonance surfaces has dimensionality $N-R-1$. The multiple resonance domain spans over the space

region surrounding this hypersurface in which the R approximated resonance conditions Eq. (3) and the propensity rules Eq. (16) are satisfied.

Let us denote by $\mathbf{J}^r$ a point in the action space at which R resonance conditions are satisfied. To estimate the span of the resonance domain around this point, we generalize the standard procedure for $N=2$ and $R=1$ [1,13]. In that particular case, $\mathbf{J}^r$ is an isolated resonant point on the energy surface, and only the action I_1 is not an adiabatic invariant of the motion during the transient process. For $N>2$, $\mathbf{J}^r$ is in general a nonisolated point located on the hypersurface of dimensionality $N-R-1$ defined by the intersection of the R resonance surfaces and the energy surface.

To estimate the maximum size of the resonance domain, we consider a family of "frozen" Hamiltonians [14,15] obtained from the averaged Hamiltonian Eq. (12) evaluated at constant values of the external additional coordinates in the global system, $\mathbf{Q}=\mathbf{Q}_F$, and the time $t=t_F$, and with the adiabatic invariants I_i, $i=R+1,\ldots,N$, corresponding to the resonant point $\mathbf{J}^r$,

$$\bar{H}'_F = \bar{H}_{0F}(I_1,\ldots,I_R) + \epsilon \bar{V}'_F(\phi_1,\ldots,\phi_R), \tag{22}$$

where

$$\bar{H}_{0F}(I_1,\ldots,I_R) = \bar{H}_0(I_1,\ldots,I_R;I^r_{R+1}\ldots,I^r_N), \tag{23}$$

and

$$\bar{V}'_F(\phi_1,\ldots,\phi_R) = \bar{V}'(\phi_1,\ldots,\phi_R;\mathbf{Q}_F,t_F). \tag{24}$$

The values of $\mathbf{Q}_F$ and t_F are selected at maximum interaction strength, when the resonance domain reaches its maximum spread in phase space. The dynamics of the perturbed system in the proximity of the resonance actions $\mathbf{J}^r$ can be analyzed by considering an expansion in $\bar{H}'_F$ up to second order in the variation of the actions I_j with respect to their resonant values I^r_j. This gives the Hamiltonian

$$\bar{H}_p = \frac{1}{2}\sum_{i=1}^{R} G_{ii}\delta I_i^2 + \sum_{i=1}^{R}\sum_{j=i+1}^{R} G_{ij}\delta I_i \delta I_j + \epsilon \bar{V}'_F(\phi_1,\ldots,\phi_R), \tag{25}$$

with $\delta I_i = I_i - I^r_i$ and

$$G_{ij} = \left.\frac{\partial^2 \bar{H}_0}{\partial I_i\, \partial I_j}\right|_{\mathbf{I}^r}. \tag{26}$$

The maximum excursions of δI_i occur along the hypersurface defined by the separatrix that passes through the unstable fixed point $\phi^u=(\phi^u_1,\ldots,\phi^u_R)$ corresponding to the global maximum of the interaction potential $\xi\bar{V}'_F$, where ξ is the sign common to every eigenvalue of the matrix $A_{\alpha\beta}=G_{\alpha\beta}/2$, giving the quadratic form $A_{\alpha\beta}\delta I_\alpha \delta I_\beta$ in Eq. (25). As the largest spread of this separatrix is obtained at the stable fixed point $\phi^s=(\phi^s_1,\ldots,\phi^s_R)$ associated with the global minimum of the potential $\xi\bar{V}'_F$, the maximum excursions of δI_i must satisfy

$$\frac{1}{2}\sum_{i=1}^{R} G_{ii}(\delta I_i^{\max})^2 + \sum_{i=1}^{R}\sum_{j=i+1}^{R} G_{ij}\delta I_i^{\max}\delta I_j^{\max} + W^s = W^u, \tag{27}$$

where $W^u=\xi\epsilon\bar{V}'_F(\phi^u)$ and $W^s=\xi\epsilon\bar{V}'_F(\phi^s)$. Therefore the changes in the actions I_i within the resonance domain are limited in the action-change space by the R-dimensional ellipsoid Eq. (27) defined by the maximum changes $\delta I_i^{\max}$. In the action-change space of the primitive actions $\mathbf{J}$ this limiting ellipsoid is transformed according to Eq. (6), leading to maximum changes in these actions

$$\delta J_i^{\max} = \sum_{j=1}^{R} M_i^{(j)}\delta I_j^{\max}, \tag{28}$$

with $i=1,\ldots,N$. The contour of the R-dimensional hypersurface defined by Eq. (28) provides both an estimate of (a) the maximum span of the region surrounding the resonant actions $\mathbf{J}^r$ in which the propensity rules Eq. (16) are satisfied, and (b) the maximum change in the actions for trajectories with initial conditions within this region. We recall that the propensity rules implicit in a resonant domain constraint the action changes in action space to a hypersurface of dimensionality R. The expression Eq. (28) is an estimate of the maximum spread of the actions from the resonant values $\mathbf{J}^r$ over such hypersurface. For example, it is an estimate of the maximum spread of the action changes along the direction $\mathbf{M}^{(1)}$ of the resonant vector within a single resonance domain, an estimate the maximum spread of the actions on the plane defined by the resonant vectors $\mathbf{M}^{(1)}$ and $\mathbf{M}^{(2)}$ within a double-resonance domain, and so on.

Our analysis assumes that there are not additional resonances in the phase space region enclosed by the estimated limiting contour of the resonance domain. The overlap of different resonance domains makes the regions where their respective propensity rules hold to shrink and eventually disappear. This demise of the resonance domains may occur due to (a) the increase in the strength of the external interaction, since it makes the resonance domains to expand and eventually collide, and (b) the progressive activation of higher order resonances in a system perturbated by a longer lasting transient interaction.

IV. THREE TRANSIENTLY COUPLED ANHARMONIC OSCILLATORS

To illustrate our previous analysis we consider a system of three anharmonic oscillators described by the Hamiltonian,

$$H_0(\mathbf{J}) = \sum_{i=1}^{3}(aJ_i - bJ_i^2), \tag{29}$$

where $\mathbf{J}=(J_1,J_2,J_3)$ and $\mathbf{\Phi}=(\Phi_1,\Phi_2,\Phi_3)$ are the action-angle variables, and with the constants $a,b>0$. This classical three anharmonic oscillators Hamiltonian has been used, for instance, in the semiclassical analysis of Bose-Einstein condensates [17]. We assume that the three-dimensional system is perturbed by an nonautonomous interaction

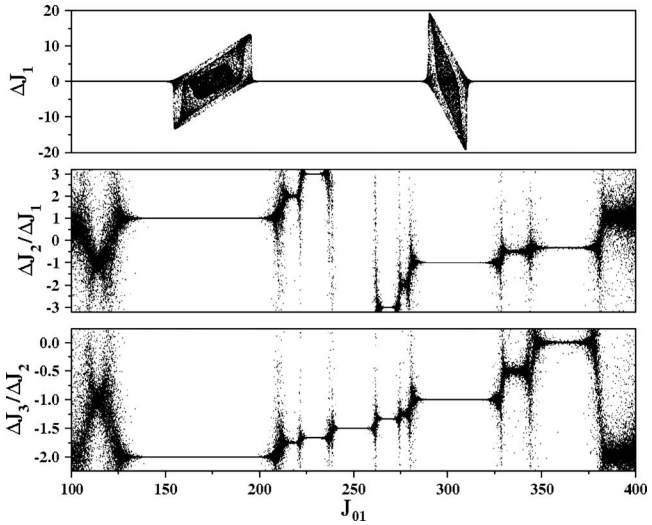

FIG. 1. The action change ΔJ_1 and the ratio of action changes $\Delta J_2/\Delta J_1$, and $\Delta J_3/\Delta J_2$ as a function of the initial action J_{01}. The initial values of the actions are taken along the straight line Eq. (32). This straight line is perpendicular to the plane defined by the resonance $\mathbf{M}^{(1)}$ and intersects this plane at $J_{01}=300$. The intersection with the plane of the resonance $\mathbf{M}^{(2)}$ occurs at $J_{01}=175$. Each point in the figure was obtained from the time evolution of trajectories from $t_i=-12\sigma$ to $t_f=12\sigma$. For each action value J_{01}, ten trajectories with initial angle variables chosen at random are included. Arbitrary units are used.

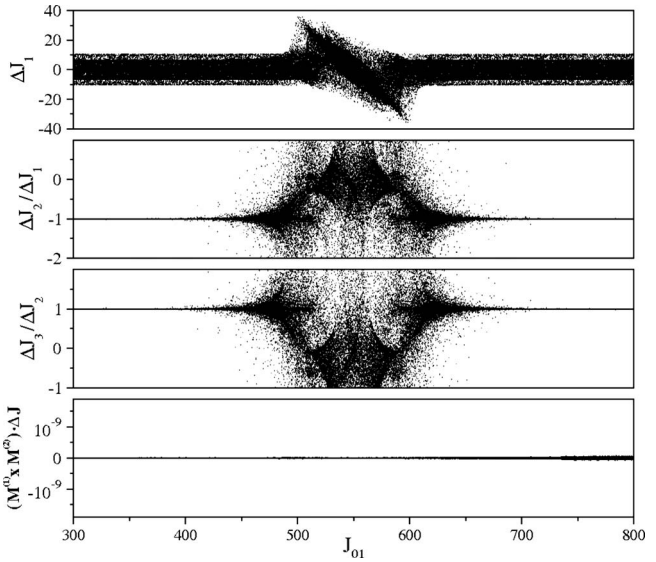

FIG. 2. The action change ΔJ_1, the ratio of action changes $\Delta J_2/\Delta J_1$ and $\Delta J_3/\Delta J_2$, and the product $(\mathbf{M}^{(1)}\times\mathbf{M}^{(2)})\cdot\Delta\mathbf{J}$ as a function of J_{01} for trajectories with initial actions taken along the straight line Eq. (33). This straight line is on the plane defined by the resonance $\mathbf{M}^{(1)}$ and intersects the plane of the resonance $\mathbf{M}^{(2)}$ at $J_{01}=550$. Each point in the figure was obtained from the time evolution of trajectories from $t_i=-12\sigma$ to $t_f=12\sigma$. For each action value J_{01}, ten trajectories with initial angle variables chosen at random have been considered. Arbitrary units are used.

$$V(\mathbf{\Phi},t)=v_0 g(t)[\sin(\mathbf{M}^{(1)}\cdot\mathbf{\Phi})+\sin(\mathbf{M}^{(2)}\cdot\mathbf{\Phi})], \quad (30)$$

with $\mathbf{M}^{(1)}=(1,-1,1)$ and $\mathbf{M}^{(2)}=(1,1,-2)$. This particular choice for the dependence of the coupling interaction on the angle variables privileges the resonance conditions $\mathbf{M}^{(1)}\cdot\boldsymbol{\omega}=0$ and $\mathbf{M}^{(2)}\cdot\boldsymbol{\omega}=0$, each of them defining a plane in the frequency space. The external interaction is turned on and off by means of the time-dependent Gaussian function

$$g(t)=e^{-(t-t_0)^2/2\sigma^2}. \quad (31)$$

In the numerical simulations we take the oscillator constants $a=1$, $b=0.001$, the interaction strength $v_0=0.3$, and the Gaussian parameters $t_0=0$ and $\sigma=50$. Arbitrary units are used throughout this section.

A. Propensity rules

Figure 1 illustrates the action change ΔJ_1 and the ratio of action changes $\Delta J_i/\Delta J_j$ for trajectories with initial actions $\mathbf{J}_0$ taken along the straight line in the frequency space

$$\omega_2=-\omega_1+\tilde{\omega}_1+\tilde{\omega}_2,$$

$$\omega_3=\omega_1-\tilde{\omega}_1+\tilde{\omega}_3, \quad (32)$$

with $\tilde{\boldsymbol{\omega}}=(0.4,0.7,0.3)$. This figure clearly shows the significant changes in the actions within the two domains associated with the isolated resonances $\mathbf{M}^{(1)}$ and $\mathbf{M}^{(2)}$. The plateau centered at the resonant action $J_{01}=175$ illustrates the three propensity rules, $\Delta J_1-\Delta J_2\approx 0$, $2\Delta J_2+\Delta J_3\approx 0$, and $2\Delta J_1+\Delta J_3\approx 0$, obtained from Eq. (16) in the proximity of the resonance $\mathbf{M}^{(2)}$. The plateau around the action $J_{01}=300$ manifests the three propensity rules, $\Delta J_1+\Delta J_2\approx 0$, $\Delta J_2+\Delta J_3\approx 0$, and $\Delta J_1-\Delta J_3\approx 0$, given by Eq. (16) in the proximity of the resonance $\mathbf{M}^{(1)}$. The figure also shows some narrow plateaus which indicate the intersection of the reference straight line Eq. (32) with additional resonant planes. For example, the resonance region centered at $J_{01}=268.75$, giving the propensity rules $3\Delta J_1+\Delta J_2\approx 0$, $4\Delta J_2+3\Delta J_3\approx 0$, and $4\Delta J_1-\Delta J_3\approx 0$, is associated with the resonance $\mathbf{M}=(1,-3,4)$, the resonance domain centered at $J_{01}=250$, with propensity rules $3\Delta J_2+2\Delta J_3\approx 0$ and $\Delta J_1\approx 0$, corresponds to the resonance $\mathbf{M}=(0,-2,3)$, and so on.

In Fig. 2 we show the action change ΔJ_1, the action-change ratios $\Delta J_i/\Delta J_j$ and the product $\mathbf{M}^{(1)}\wedge\mathbf{M}^{(2)}\wedge\Delta\mathbf{J}=(\mathbf{M}^{(1)}\times\mathbf{M}^{(2)})\cdot\Delta\mathbf{J}$ for trajectories with initial actions $\mathbf{J}_0$ fixed along the straight line in the frequency space

$$\omega_2=2\omega_1-2\tilde{\omega}_1+\tilde{\omega}_2,$$

$$\omega_3=\omega_1-\tilde{\omega}_1+\tilde{\omega}_3. \quad (33)$$

The figure clearly shows the double-resonance domain with larger action changes centered at the initial action $J_{01}=550$. In this region the three propensity rules corresponding to the single resonance $\mathbf{M}^{(1)}$ break down and only the propensity rule given by Eq. (16) for the double resonance, $\mathbf{M}^{(1)}\wedge\mathbf{M}^{(2)}\wedge\Delta\mathbf{J}\approx 0$, is satisfied. We recall that the three propensity rules corresponding to the single resonance imply that $\mathbf{M}^{(1)}\wedge\Delta\mathbf{J}=\mathbf{M}^{(1)}\times\Delta\mathbf{J}\approx 0$. Therefore the product $(\mathbf{M}^{(1)}\times\mathbf{N})\cdot\Delta\mathbf{J}\approx 0$ is also satisfied in the single resonance domain for any vector $\mathbf{N}$.

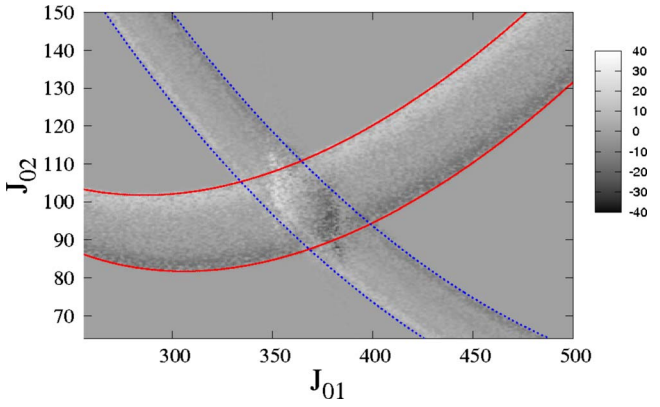

FIG. 3. (Color online) Contour map of the action change ΔJ_1 versus the initial actions J_{01} and J_{02} for a system with constant initial energy $E_0=500$ (the initial value of the action J_3 is fixed by the condition of constant energy). The two paths in the figure illustrate the domains of the isolated resonances $M^{(1)}$ (from up right to down left) and $M^{(2)}$ (from up left to down right). In the overlap between both paths, larger action changes occur due to the double-resonance condition. The red solid and the blue dashed lines indicate the estimated limits of each single resonance domain, derived from Eq. (28) for $N=3$ and $R=1$. Arbitrary units are used.

B. Span of the resonance domains

The results presented in Figs. 1 and 2 to illustrate the propensity rules arising in the proximity of a single and a double resonance were obtained considering trajectories with initial actions $\mathbf{J}_0$ corresponding to different initial energies $E_0=H_0(\mathbf{J}_0)$. In this section, in order to check our estimate of the size of a resonance domain, we restrict our analysis to trajectories with initial actions selected on the same energy surface.

Figure 3 displays a contour map of the action change ΔJ_1 for trajectories with the same initial energy. The changes in the actions J_2 and J_3 (not depicted in the figure) present a similar behavior. The figure shows the two paths reflecting the significant action changes occurring within the domain of each isolated resonance $\mathbf{M}^{(1)}$ and $\mathbf{M}^{(2)}$. The larger action changes in the region defined by the intersection of the two resonances can also be distinguished. The estimated limits of each isolated resonance domain are also shown.

Figure 4 shows the distributions of the final actions corresponding to different ensembles of trajectories with initial actions taken within the single and double-resonance domains. Within the single resonance domains the action changes are aligned along the corresponding resonance vector in the action-change space, as the propensity rule $\mathbf{M}^{(i)}\wedge\Delta\mathbf{J}\approx 0$ imposes. This implies that the final action values are also aligned in the (J_1,J_2) plane depicted in the figure. Within the double-resonance domain the action changes spread over the plane defined by the two resonance vectors in the action-change space, according to the propensity rule $\mathbf{M}^{(1)}\wedge\mathbf{M}^{(2)}\wedge\Delta\mathbf{J}\approx 0$. In the figure this is reflected by the spread of the final action values within the multiple resonance domain.

V. DIATOM-DIATOM COLLISIONS

In this section we analyze the inelastic collision between two vibro-rotationally excited diatomic molecules. In the

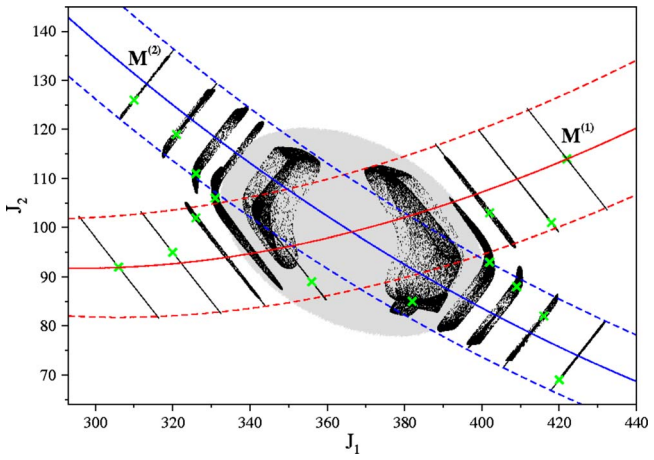

FIG. 4. (Color online) The distributions of the final actions for different ensembles of trajectories with initial actions within the single and double-resonance domains depicted in Fig. 3. In each ensemble we consider 2×10^4 trajectories with the same initial actions (the green crosses) and with initial angle variables fixed at random. The solid lines are the exact single resonance curves $\mathbf{M}^{(1)}$ and $\mathbf{M}^{(2)}$, the surrounding dashed lines indicate the estimated span of their domains. The elliptical gray shaded area is the estimated span of the double-resonance domain obtained from Eq. (28) for $N=3$ and $R=2$. Arbitrary units are used.

frame of the global center of mass, the Hamiltonian of the system can be written as

$$H=\sum_{\alpha=1}^{2}\left[\frac{p_{r\alpha}^2}{2m_\alpha}+\frac{l_\alpha^2}{2m_\alpha r_\alpha^2}+U_\alpha(r_\alpha)\right]+\frac{P_r^2}{2m}+\frac{L^2}{2mr^2}+V(\mathbf{r}_1,\mathbf{r}_2,\mathbf{r}), \tag{34}$$

where r_α is the interatomic distance in each molecule, $p_{r\alpha}$ its conjugated momentum, r is the distance between the centers of mass of the two molecules, P_r its conjugate momentum, m_α is the reduced mass of each molecule, m the reduced mass of the two molecules, $\mathbf{l}_\alpha=l_\alpha\hat{\mathbf{l}}_\alpha$ is the angular momentum of each molecule, and $\mathbf{L}=L\hat{\mathbf{L}}$ is the orbital angular momentum of the relative motion between the two molecules. For the sake of simplicity we confine the collision process to a plane by setting the two molecular angular momenta and the orbital angular momentum along the same direction.

The response of the four-dimensional system composed by the two isolated molecules to the transient perturbation, due to their interaction during the collision, depends on the resonance conditions that the internal molecular frequencies may satisfy. The unperturbed system

$$H_0(\mathbf{J})\equiv H_0(J_{v1},J_{r1},J_{v2},J_{r2})=\sum_{\alpha=1}^{2}H_{0\alpha}(J_{v\alpha},J_{r\alpha}) \tag{35}$$

has well-defined vibrational (radial) and rotational (angular) action variables,

$$J_{v\alpha} = \frac{1}{2\pi}\oint p_{r\alpha} dr_\alpha = \frac{1}{2\pi}\oint \sqrt{2m_\alpha[E_{0\alpha} - U_\alpha(r_\alpha)] - \frac{l_\alpha^2}{r_\alpha^2}} dr_\alpha \tag{36}$$

and

$$J_{r\alpha} = \frac{1}{2\pi}\oint l_\alpha d\theta_\alpha = l_\alpha, \tag{37}$$

with θ_α the angular coordinate of each molecule and $E_{0\alpha}$ their internal energy. A detailed description of classical (di)atom-diatom collisions in terms of vibro-rotational action-angle variables used for the direct numerical integration of the equations of motion is given in Ref. [18].

A resonance condition in this system

$$\mathbf{M}\cdot\omega \equiv M_{v1}\omega_{v1} + M_{r1}\omega_{r1} + M_{v2}\omega_{v2} + M_{r2}\omega_{r2} = 0, \tag{38}$$

where $\omega_{v\alpha} = \partial H_{0\alpha}/\partial J_{v\alpha}$ and $\omega_{r\alpha} = \partial H_{0\alpha}/\partial J_{r\alpha}$, may involve just the two internal frequencies of one molecule (*intramolecular* resonance), or include internal frequencies of both molecules (*intermolecular* resonance). The collisions occurring from initial states within a single intramolecular resonance domain can only induce action changes in the nearly resonant molecule, giving the propensity rule $M_r\Delta J_v - M_v\Delta J_r \approx 0$. Therefore the response of this molecule would be equivalent to one arising in the atom-diatom collisions [16]. The effects associated with a intermolecular resonance can induce changes in the actions of both molecules. Meanwhile a multiple resonant system might involve any combination of intermolecular and intramolecular resonances.

We simulate the H_2+H_2 collision considering the H_2 potential of Schwenke [19] and the H_2-H_2 interaction potential proposed by Billing [20]. As occurs in the atom-diatom collisions, the robustness of the effects arising in the nearly resonant molecules with respect to the details of the interaction potential between the colliding species justifies the use of this simple model. We choose the collision energy $E=3\times10^{-6}$ a.u., which is above a factor of 30 smaller than the attractive well in the interaction potential between the two molecules. Throughout this section atomic units are used.

Figure 5 displays a contour map of the action changes ΔJ_{v1} and ΔJ_{r1} in the collisions H_2+H_2 for different initial rotational actions (J_{r1},J_{r2}). The action changes ΔJ_{v2} and ΔJ_{r2} (not depicted in the figure) present a similar behavior. The figure illustrates the action changes for initial molecular states within different molecular resonance domains. The curves corresponding to the exactly resonance conditions are labeled in Fig. 6.

The most significant molecular response arises in the proximity of the intramolecular resonance $(1,-2,0,0)$, which can give action changes up to one order of magnitude higher than the other resonances. This resonance is responsible for the dominant resonant effect in the $He+H_2$ collisions [16,21]. The intramolecular resonance $(1,-4,0,0)$ also leads to appreciable action changes.

In addition to the intramolecular resonances, the combined molecular responses in the proximity of some intermolecular resonances are also activated. We can see the action

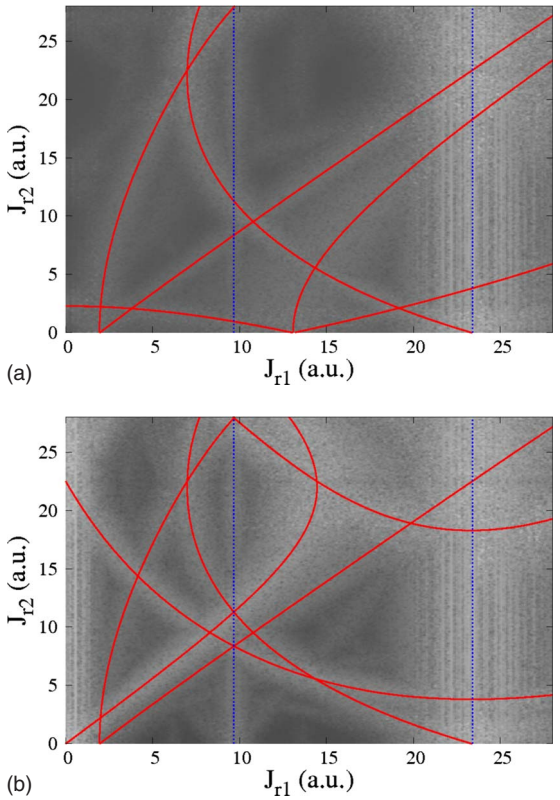

FIG. 5. (Color online) Contour map of the change in the vibrational (upper panel) and rotational (lower panel) actions (J_{v1},J_{r1}) versus the two initial rotational actions in the collision H_2+H_2. The initial vibrational actions were chosen to satisfy the semiclassical quantization rule $J_{v\alpha}=\hbar(v_\alpha+1/2)$, with vibrational quantum numbers $v_1=0$ and $v_2=2$. The collision energy is $E=3\times10^{-6}$ a.u. For each (J_{r1},J_{r2}) we compute a classical collision trajectory with random initial angle variables and impact parameter $|b|\leq 2$ a.u. The values of the action changes are scaled by $\Delta J \rightarrow |\Delta J|^{1/3}$ for better color contrast, white is largest and black is smallest. The red solid lines are intermolecular resonance curves and the blue dashed vertical lines intramolecular resonances. The depicted molecular resonance curves are labeled in Fig. 6.

changes associated with the pure-rotational resonance $(0,1,0,-1)$, which leads to the correlation $\Delta J_{1r}+\Delta J_{2r}\approx 0$ between the two molecular rotational actions, and practically no change in the vibrational actions. The correlation $\Delta J_{1v}+\Delta J_{2v}\approx 0$ between the two vibrational actions and the adiabatic invariance of the two rotational actions arises within the domain of the pure-vibrational resonance $(1,0,-1,0)$. An intermolecular rotation-vibration action exchange occurs in the proximity of the resonance $(0,2,-1,0)$, which gives rise to the propensity rule $\Delta J_{1r}+2\Delta J_{2v}\approx 0$ and the adiabaticity of the actions J_{1v} and J_{2r}. Other intermolecular resonances giving an appreciable response involve three molecular frequencies, such as the resonance $(0,2,-1,2)$ leading to the adiabatic invariance of the action J_{1v} and action changes that satisfy the propensity rules $\Delta J_{1r}+2\Delta J_{2v}\approx 0$, $\Delta J_{1r}-\Delta J_{2r}\approx 0$, and $2\Delta J_{2v}+\Delta J_{2r}\approx 0$. Also the action changes associated with the four-frequency resonance $(1,-2,-1,2)$ can be distinguished. Within this single resonance domain, the adiabatic invariance of the three actions $I_1=2J_{1v}+J_{1r}$, $I_2=J_{1v}+J_{2v}$, and

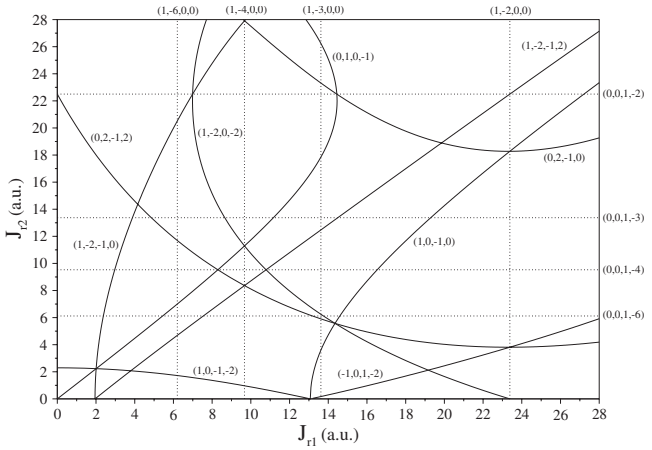

FIG. 6. The map of the molecular resonances $(M_{v1},M_{r1},M_{v2},M_{r2})$ associated with the more significant changes in the vibrational and rotational actions presented in Fig. 5. The dashed lines are the intramolecular resonances, the solid lines are the intermolecular resonance curves.

$I_2=-2J_{1v}+J_{2r}$ determine six different propensity rules relating the changes in the vibrational and rotational actions of both molecules.

So far we have mentioned the propensity rules arising within the more relevant single resonance domains activated by the interaction between the two molecules. As it was shown in the three oscillators model, the overlap of different resonance domains demises their respective adiabatic invariants and spawns new ones leading to a reduced number of propensity rules. To illustrate this multiple resonance effect in the diatom-diatom collisions, we analyze the action changes and the different adiabatic invariants arising along an specific resonance. Since we are dealing with a four-dimensional system, in a multiple resonance domain only up to three of the intersecting resonance conditions are linearly independent. Figure 7 displays the change in the four molecular actions for classical trajectories with initial conditions taken along the pure-rotational resonance $(0,1,0,-1)$. In Fig. 8 we show the changes in the actions corresponding to the adiabatic invariants arising from some of the intersections with other resonances, see Fig. 6. There are three main regions in which the propensity rules derived from the three adiabatic invariants, $I_1=J_{1v}$, $I_2=J_{2v}$, and $I_3=J_{1r}+J_{2r}$, associated with this single resonance are totally or partially destroyed and new ones arise. As the initial value of the action J_{2r} increases, we can see: (a) The triple resonance domain given by the intersection with the resonances (0,0,0,1) and $(1,-2,-1,0)$, leading to the adiabatic invariance of the single action $I_a=J_{1v}+J_{2v}$, (b) the triple resonance domain defined by the intersection with the two intramolecular resonances $(0,0,1,-4)$ and $(1,-4,0,0)$, in which the single adiabatic invariant $I_b=4J_{1v}+J_{1r}+4J_{2v}+J_{2r}$ arises, and (c) the triple resonance domain defined by the intersection with the intramolecular resonances $(0,0,1,-2)$ and $(1,-3,0,0)$, which gives rise to the adiabatic invariance of the single action $I_c=3J_{1v}+J_{1r}+2J_{2v}+J_{2r}$.

On both sides of the triple resonance domain (b) the three adiabatic invariants arising from the reference resonance are

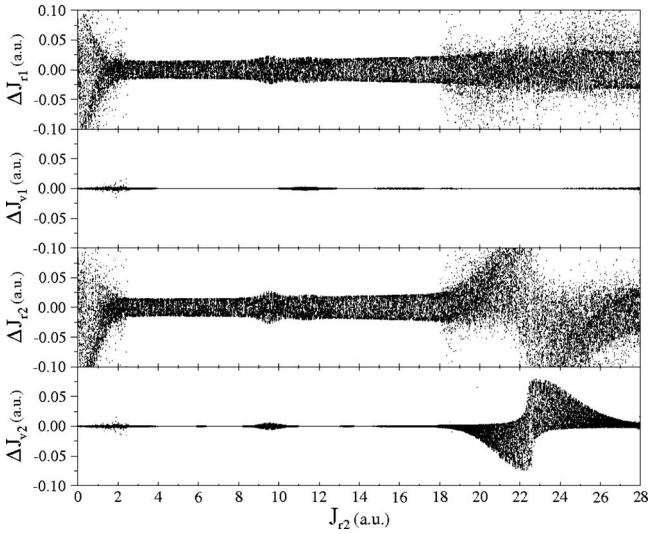

FIG. 7. The changes in the vibrational and rotational molecular actions for trajectories with initial rotational actions (J_{r1},J_{r2}) selected along the curve of the pure-rotational resonance $(0,1,0,-1)$ depicted in Fig. 6. The collision trajectories were computed as described in Fig. 5. Each value of J_{r2} include the results of seven trajectories.

only partially destroyed due to its intersection with one of the intramolecular resonances. At lower initial values of J_{2r}, the double-resonance domain defined by the intersection with the resonance $(0,0,1,-4)$ preserves the adiabatic invariance of the two actions $I_1=J_{1v}$ and $I_2=J_{1r}+4J_{2v}+J_{2r}$. Meanwhile, the intersection with the resonance $(1,-4,0,0)$ at upper initial values of J_{2r} defines a double-resonance domain leading to the two adiabatic invariants $I_1=J_{2v}$ and $I_2=4J_{1v}+J_{1r}+J_{2r}$.

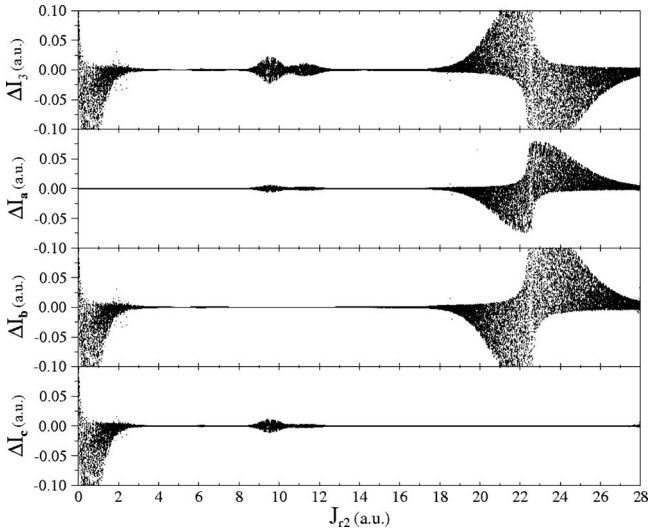

FIG. 8. The change in the actions corresponding to some of the adiabatic invariants arising from the classical trajectories depicted in Fig. 7. $I_3=J_{1r}+J_{2r}$, $I_a=J_{1v}+J_{2v}$, $I_b=4J_{1v}+J_{1r}+4J_{2v}+J_{2r}$, and $I_c=3J_{1v}+J_{1r}+2J_{2v}+J_{2r}$.

VI. CONCLUSIONS

The response of a nearly resonant multidimensional system to a weak transient perturbation has been studied. Assuming a slowly variant interaction acting on a system with well-defined initial actions, it cannot always be turned on and off so slowly that all the internal coordinates become adiabatic. Indeed resonances or near resonances in the system may spawn extremely slow coordinates with effectively zero frequency, and which therefore fail to be adiabatic. But the interaction may still be slow compared to some of the remaining coordinates, which may be fast enough to have conserved actions. In that case, a canonical transformation into the resonant slow and fast angles reveals the specific form of the adiabatic actions corresponding to the fast angles in the proximity of each resonance. The resonant transformation dictates the linear relations giving the adiabatic invariants in terms of primitive actions in the unperturbed system, and which determine the strong correlations observed between the changes in the actions.

In the phase space of the system, the significant action changes in the proximity of a resonance condition are connected with the demise of the rational tori bearing the resonant frequencies, in which such actions are adiabatic invariants, and the emerge of a strong nonlinear resonance zone in which new resonant adiabatic invariants may arise. The spread of the actions throughout the phase-space region visited by this resonance zone make possible the significant changes in the initial actions. Moreover, although the structures in phase space are always changing during the transient interaction, the analysis of their time evolution becomes particularly useful for estimating the span of the interval of initial states defining the resonance domain in which the strong correlations between the action changes persist. In any case, we are considering transient processes in which the duration of the external interaction is not long enough to induce the large excursions of the actions along the resonance zones characterizing the Arnold diffusion in multidimensional systems.

The classical analysis of nearly resonant systems under a transient perturbation has been applied to low energy atom-diatom collisions in Refs. [16,21]. Although the action changes obtained in these processes are always much smaller than a single quantum, the comparison with the corresponding quantum rate coefficients has shown that the classical treatment provides at least a rough estimate of the system response [21]. In this work we study the low energy collisions between two H_2 molecules in the context of the generalized classical analysis for multidimensional system. Our results indicate that the initial molecular actions leading to significant action changes are associated with low order intramolecular and intermolecular resonance domains. The most relevant molecular response corresponds to the same intramolecular rotation-vibration exchange that gives to most remarkable peak in the vibro-rotational inelastic rate constant in the H_2+He collisions. As in this scattering process, the action changes obtained in the low energy regime do not reach a single quantum. However, the collisions between two diatom molecules present some aspects which are absent in the atom-diatom collisions. In the diatom-diatom collisions, the overlap of the intramolecular resonances with different intermolecular resonance domain(s) destroys the adiabatic invariants associated with the single resonances and introduce the corresponding multiple resonance adiabatic invariants. Besides, system responses involving intermolecular action exchanges, such as rotation-rotation and vibration-vibration action exchanges, or more complicated combinations including the rotational and vibrational actions of both molecules can be activated. These molecular action exchange mechanisms could be relevant in processes such as the cooling and trapping of molecules [22], in which the intermolecular inelastic processes could compete with the cooling mechanisms, or in the energy transfer in ultracold molecule-molecule collisions [23].

In summary, we have shown the general expression for the propensity rules relating the action changes that a weak transient perturbation can induce in a classical system with initial state within the domain of a single resonance or within the domain defined by the overlap of multiple resonances. Although the response of the nearly resonant system to the perturbation may cause significant changes in the actions, the internal energy is approximately preserved throughout the interaction. An estimate of the span of single resonance domains and multiple intersecting resonance domains have been also obtained. Numerical simulations for a system of three anharmonic oscillators and diatom-diatom collisions illustrate our main results.

ACKNOWLEDGMENTS

This work was supported by Spanish MCT (Grant No. FIS2007-64018). A.R. thanks Daniel Alonso for fruitful discussions.

[1] V. I. Arnold, V. V. Kozlov, and A. I. Neishtadt, *Mathematical Aspects of Classical and Celestial Mechanics* (Springer-Verlag, Berlin, 2006).

[2] B. Stewart, P. D. Magill, T. P. Scott, J. Derouard, and D. E. Pritchard, Phys. Rev. Lett. **60**, 282 (1988).

[3] P. D. Magill, B. Stewart, N. Smith, and D. E. Pritchard, Phys. Rev. Lett. **60**, 1943 (1988).

[4] P. D. Magill, T. P. Scott, N. Smith, and D. E. Pritchard, J. Chem. Phys. **90**, 7195 (1989).

[5] T. P. Scott, N. Smith, P. D. Magill, D. E. Pritchard, and B. Stewart, J. Phys. Chem. **100**, 7981 (1996).

[6] P. Rousseau, H. Khemliche, A. G. Borisov, and P. Roncin, Phys. Rev. Lett. **98**, 016104 (2007).

[7] A. Schüller, S. Wethekam, and H. Winter, Phys. Rev. Lett. **98**, 016103 (2007).

[8] A. Schüller and H. Winter, Phys. Rev. Lett. **100**, 097602

(2008).
[9] N. Bundaleski, H. Khemliche, P. Soulisse, and P. Roncin, Phys. Rev. Lett. **101**, 177601 (2008).
[10] A. Schüller, M. Busch, S. Wethekam, and H. Winter, Phys. Rev. Lett. **102**, 017602 (2009).
[11] A. Ruiz, J. P. Palao, and E. J. Heller, J. Phys.: Conf. Ser. **99**, 012018 (2008).
[12] A. Ruiz, J. P. Palao, and E. J. Heller, Phys. Rev. A **79**, 052901 (2009).
[13] A. J. Lichtenberg and M. A. Lieberman, *Regular and Chaotic Dynamics* (Springer-Verlag, New York, 1992).
[14] W. J. Hoving and R. Parson, Chem. Phys. Lett. **158**, 222 (1989).
[15] A. Ruiz and E. J. Heller, Mol. Phys. **104**, 127 (2006).
[16] A. Ruiz and E. J. Heller, J. Phys. Chem. A **109**, 11578 (2005).
[17] S. Mossmann and C. Jung, Phys. Rev. A **74**, 033601 (2006).
[18] N. Smith, J. Chem. Phys. **85**, 1987 (1986).
[19] D. W. Schwenke, J. Chem. Phys. **89**, 2076 (1988).
[20] G. D. Billing, Chem. Phys. **20**, 35 (1977).
[21] R. C. Forrey, N. Balakrishnan, A. Dalgarno, M. R. Haggerty, and E. J. Heller, Phys. Rev. Lett. **82**, 2657 (1999).
[22] R. C. Forrey, Phys. Rev. A **63**, 051403(R) (2001).
[23] G. Quéméner, N. Balakrishnan, and R. V. Krems, Phys. Rev. A **77**, 030704(R) (2008).